Naval Research Laboratory

Washington, DC 20375-5320

NRL/MR/5708--20-10,100

Experimental Proof of Concept for Heat Sink-Controlled Temperature Fields within Multi-Layered Materials

Edward PA Michaelchuck, Jr.

Scott A. Ramsey

Troy Mayo

Signature Technology Office
Tactical Electronic Warfare Division

Samuel G. Lambrakos

Center for Materials Physics & Technology Branch
Materials Science & Technology Division

October 11, 2020

REPORT DOCUMENTATION PAGE

Form Approved
OMB No. 0704-0188

1. REPORT DATE *(DD-MM-YYYY)*
11-10-2020

2. REPORT TYPE
NRL Memorandum Report

3. DATES COVERED *(From - To)*

4. TITLE AND SUBTITLE

Experimental Proof of Concept for Heat Sink-Controlled Temperature Fields within Multi-Layered Materials

5a. CONTRACT NUMBER

5b. GRANT NUMBER

5c. PROGRAM ELEMENT NUMBER

6. AUTHOR(S)

Edward PA Michaelchuck, Jr., Scott A. Ramsey, Troy Mayo, and Samuel G. Lambrakos

5d. PROJECT NUMBER

5e. TASK NUMBER
0010

5f. WORK UNIT NUMBER
100001558391

7. PERFORMING ORGANIZATION NAME(S) AND ADDRESS(ES)

Naval Research Laboratory
4555 Overlook Avenue, SW
Washington, DC 20375-5320

8. PERFORMING ORGANIZATION REPORT NUMBER

NRL/MR/5708--20-10,100

9. SPONSORING / MONITORING AGENCY NAME(S) AND ADDRESS(ES)

US Special Operations Command, Special Operations Forces Acquisition, Technology, and Logistics
MacDill AFB
Tampa, FL 33621

10. SPONSOR / MONITOR'S ACRONYM(S)

USSOCOM SOF AT&L

11. SPONSOR / MONITOR'S REPORT NUMBER(S)

12. DISTRIBUTION / AVAILABILITY STATEMENT

DISTRIBUTION STATEMENT A: Approved for public release; distribution is unlimited.

13. SUPPLEMENTARY NOTES

14. ABSTRACT

This report describes a series of experiments that provide proof of concept for heat sink control of temperature fields within multi-layer materials consisting of a fabric and conductive substrate. The primary focus of this experiment is to observe the effects of coupling fabrics with heat sinks. By building layered fabric materials that include a heat sink layer, the surface temperature may be controlled via a system not centralized to the location of the desired cooling. This kind of layered material that can transfer heat to a centralized location can be desirable for designing clothing with cooling capabilities. These experiments are not for demonstrating optimal materials for heat sink thermal control, but rather to demonstrate the feasibility of such control using work piece fabrics and heat sink materials, which are realistic and have sufficiently different thermal diffusivities.

15. SUBJECT TERMS

Heat sink Layered materials Temperature fields
Heat transfer Thermal control

16. SECURITY CLASSIFICATION OF: a. REPORT	b. ABSTRACT	c. THIS PAGE	17. LIMITATION OF ABSTRACT	18. NUMBER OF PAGES	19a. NAME OF RESPONSIBLE PERSON
					Edward Michaelchuck
Unclassified Unlimited	Unclassified Unlimited	Unclassified Unlimited	Unclassified Unlimited	14	**19b. TELEPHONE NUMBER** *(include area code)* (202) 279-5233

Standard Form 298 (Rev. 8-98)
Prescribed by ANSI Std. Z39.18

This page intentionally left blank.

Table of Contents

This page intentionally left blank.

Introduction

The need to control heat transfer through multilayer materials is ubiquitous and multidisciplinary with respect to applications. These applications range from control of volumetric heat deposition for surface treatment of materials to thermal management of systems which work to eliminate, localized high-temperature regions to maintain system integrity. Optimizing heat transfer through multilayer materials requires estimating the thermal response of layered composite materials, whose fabrication is both feasible and operationally practical. Accordingly, material designs that combine heat-transfer characteristics and thermal material properties, enabling optimization of temperature fields within multilayer materials should be well posed. These designs should be conveniently adaptable for controlling the thermal response of different types of layered materials.

A general approach for control of heat transfer through multilayer materials is that of system design which includes heat sinks as coupled or embedded layers. The general physical character of heat sinks is that their thermal diffusivities are substantially greater than those of work pieces (i.e. fabrics, waterproof membranes, neoprenes) whose temperature fields are to be controlled. This allows for the conduction of thermal energy from the heat source to the heat sink to occur rather than passing the thermal energy to the external environment. This approach is motivated by welding processes, whereby work piece temperatures are controlled by thermal contact to base plates and by electronic system designs requiring thermal management. [1]

This report describes a series of experiments that provide proof of concept for heatsink-control of temperature fields within multi-layer materials consisting of a fabric and a thermally conductive substrate. The primary objective of this experiment is to observe the effects of coupling a fabric layer with a heatsink. By building layered fabric materials that include a heatsink layer, the surface temperature may be controlled via a system not centralized to the location of the desired cooling. This kind of layered material that can transfer heat to a centralized location can be desirable for designing clothing with cooling capabilities. Note that these experiments are not for demonstrating optimal materials for heatsink thermal control, but rather to demonstrate the feasibility of such control using work piece and heatsink materials, which are realistic, and have sufficiently different thermal diffusivities.

Organization of subject areas presented are as follows. First, the thermodynamic theory behind multi-layer materials is defined. Second, the experimental setup providing proof of concept for heatsink-control of temperature fields within materials are presented. Third, the results of the proof-of-concept experiment are described. Lastly, a discussion of the results is given.

Manuscript approved Month 00, 2020.

Multi-Layer Heat Transfer Theory

A uniform, multi-layer material can be treated as a two dimensional heat transfer problem, Figure 1, governed by the 2-D heat conduction equation, which is given by

$$\dot{T} = \alpha\nabla^2 T \qquad \text{Eq. 1}$$

Where T is temperature [K], α is the thermal diffusivity of the material [m^2/s], ∇ is the Laplace operator, and $\dot{T}$ is the time derivative of T. [2]

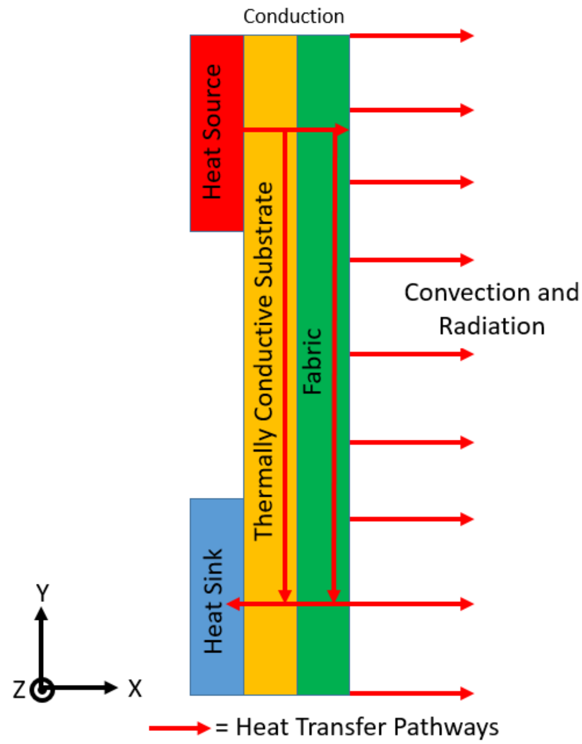

Figure 1. Two dimensional view of a multi-layer material stack consisting of a fabric and thermally conductive substrate. There are two paths for heat transfer, the XZ-plane and YZ-plane. The XZ-plane has three forms of heat transfer: conduction through the layers, convection at the outer surface, and radiative heat transfer at the outer surface. The XY-plane only has heat conduction through the materials.

This problem can be further reduced into two, perpendicular 1-D problems, where heat flows in the XZ-plane that is perpendicular to the heat source, and in YZ-plane that is parallel to the heat source. The 1-D steady state heat flux through the material is given by

$$\dot{q} = \frac{\Delta T}{R \cdot A} \qquad \text{Eq. 2}$$

Where $\dot{q}$ is the heat flux through the material [$W \cdot m^{-2}$], R is the thermal resistance of the layered material [$K \cdot W^{-1}$], A is the cross sectional area of the material [m^2], and ΔT is the temperature difference between the inner and outer surface of the material [K]. [2, 3]

In the perpendicular case, the thermal resistances of the multi-layer material are in series, Equation 3. [2, 3] In series, the thermal resistance will be dominated by the fabric layer assuming the thermal conductivity of the thermally conductive substrate is much greater than that of the fabric. The total thermal resistance of materials in series is given by

$$R = \sum_{n=0}^{N} R_n \qquad \text{Eq. 3}$$

Where R is the total thermal resistance in [$K \cdot W^{-1}$], R_n is the thermal resistance of each layer in [$K \cdot W^{-1}$], and N is the number of layers. [2, 3] The thermal resistance of an individual layer is given by

$$R_n = \frac{\tau_n}{k_n \cdot L \cdot W} \qquad \text{Eq. 4}$$

Where R_n is the thermal resistance [$K \cdot W^{-1}$], k_n is the thermal conductivity [$W \cdot m^{-1} \cdot K^{-1}$], τ_n is the thickness of the material [m], w is the width of the material [m], and L is the path length from the heat source to the cold plate [m]. [2, 3] Note that w and L are considered to be the same for each layer.

In the parallel case along the YZ-plane, the thermal resistances of the materials are in parallel, Equation 5. If the thermal conductivity of the thermally-conductive substrate dominates while in parallel, then the thermal resistance reduces to the low thermal resistivity of the thermally conductive substrate. [2, 3] The total thermal resistance for materials in parallel is given by

$$\frac{1}{R} = \sum_{n=0}^{N} \frac{1}{R_n} \qquad \text{Eq. 5}$$

Where R is the total thermal resistance in [$K \cdot W^{-1}$], R_n is the thermal resistance of each layer in [$K \cdot W^{-1}$], and N is the number of layers. The thermal resistance of an individual layer in the YZ-plane is given by

$$R_n = \frac{L}{k_n \cdot t_n \cdot w} \qquad \text{Eq. 6}$$

Where R_n is the thermal resistance [$K \cdot W^{-1}$] of each layer, k_n is the thermal conductivity [$W \cdot m^{-1} \cdot K^{-1}$] of each layer, τ_n is the thickness of the material [m] of each layer, w is the width of the material [m], and L is the path length from the heat source to the cold plate [m]. [2, 3] Note that w and L are considered to be the same for each layer.

Experimental Setup

This section presents temperature distribution experiments of a heatsink-controlled, multi-layered material consisting of a single fabric and various heatsink materials. In this experiment, the material is attached to both a hot plate and a cold plate. The goal of the experiment is to measure the material's outer surface temperature at steady state before and after the addition of a cold plate. The region of interest (ROI) for the change in temperature will be the region of the material directly over the heat source. Additionally, the specific temperature profiles from heat source to heat sink are of interest.

Shown in Figure 2 and 3 are the block diagrams of the experimental setup showing the key components in addition to the heat transfer pathways.

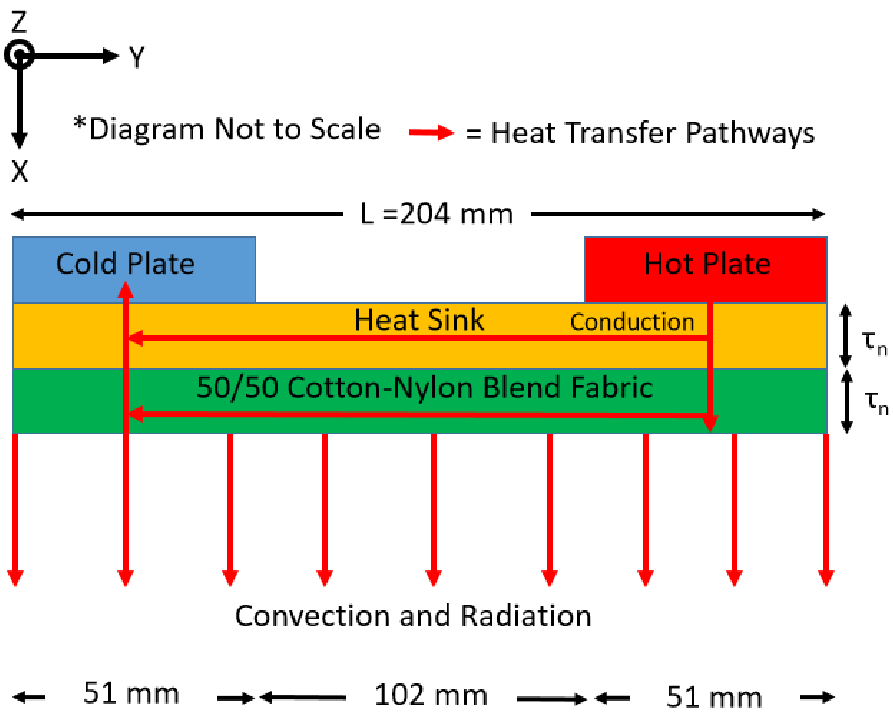

Figure 2. Top down view of a cross-sectional block diagram in the XY-plane for the experimental evaluation of multilayer fabric materials.

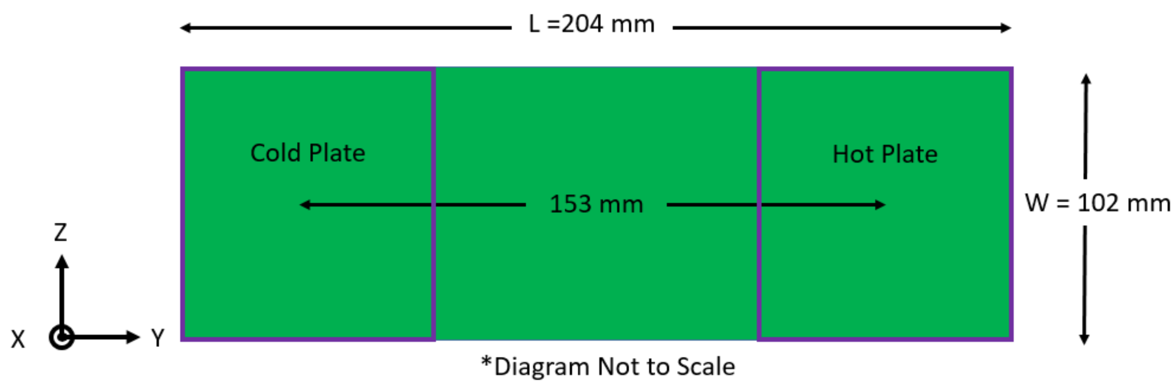

Figure 3. Front view of a cross-sectional diagram in the YZ-plane. Dimensions of the experimental setup are shown along with the locations of the hot and cold plates.

The heat transfer pathways can also be represented by two thermal circuits, Figure 4 and 5. In the XZ-plane, the thermal resistances of the materials are in series, and the heat flux passes through the layered material via conduction and expels heat to the ambient environment via radiation and convection. In the YZ-plane, the thermal resistances of the materials are in parallel, and the heat flux travels in the direction of the cold plate via conduction. Although heat transfer at the outer surface of the multi-layered material contributes significantly to the outer surface temperature, convective and radiative heat transfer are disregarded in this experiment because 1) the same fabric sample is used at the outer surface, 2) the experiment takes place in a room with HVAC where the room temperature was (~22^{O}C each day of experimentation), and 3) the IR cameras are calibrated to a set of blackbodies. Since the outer surface effects are being disregarded in this analysis, the thermal resistivity circuit loses the convection and radiation components.

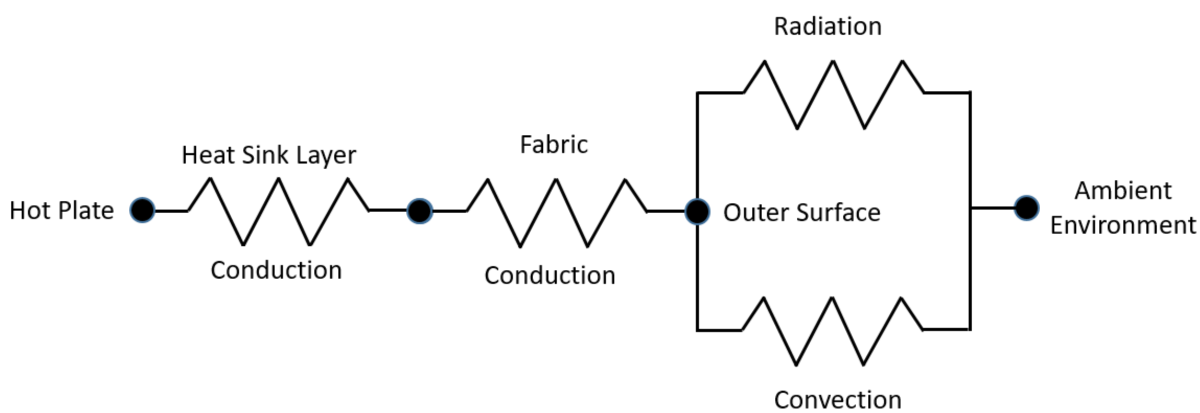

Figure 4. Thermal circuit diagram in the XZ-plane. The materials are in series.

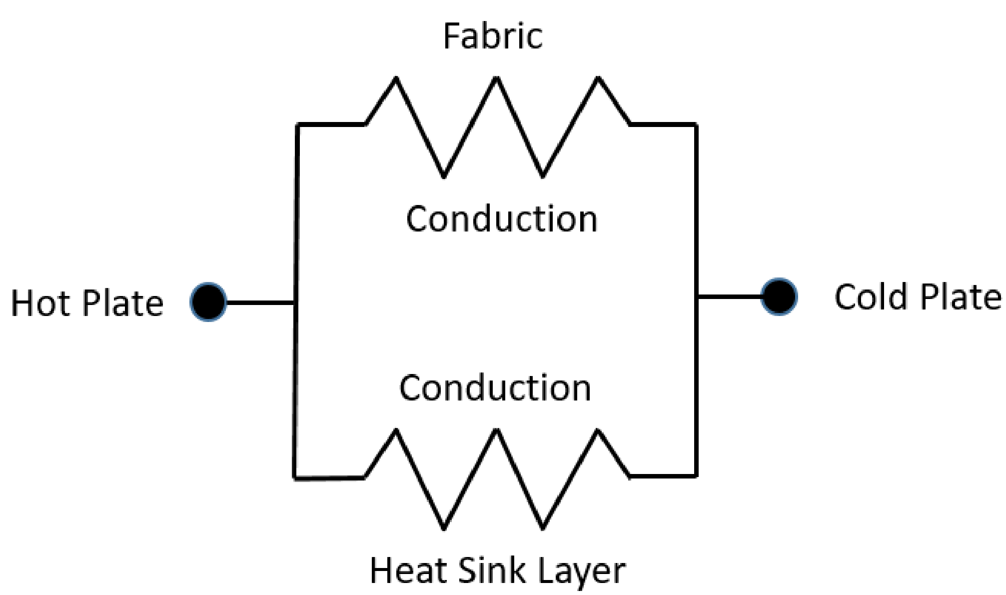

Figure 5. Thermal circuit diagram in the YZ-plane. The materials are in parallel.

Experimental Housing and IR Imaging

A housing constructed with R10 insulation was used as the housing for all experimentation. A thermal infrared (IR) image of the experimental setup is shown in Figure 6. The heat source, having an approximate temperature of 38°C and a total power output of 17 Watts over a 1ft^2 area, was installed on the right-hand side, and a cold plate (heat sink) consisting of a frozen gel ice pack with an approximate temperature of -10 °C was installed on the left. The gel ice pack is a smooth rectangular shape (102mm L x 25.4mm W x 102mm H). The multi-layer material (204mm L x 102mm W) that couples the heat sink and heat source consists of a 50/50 Cotton/Nylon blend ripstop weave fabric outer layer, and one of three types of extremely thin conductive metal film (~20-30 µm thickness) of either copper, aluminum, or graphite as the inner layer.

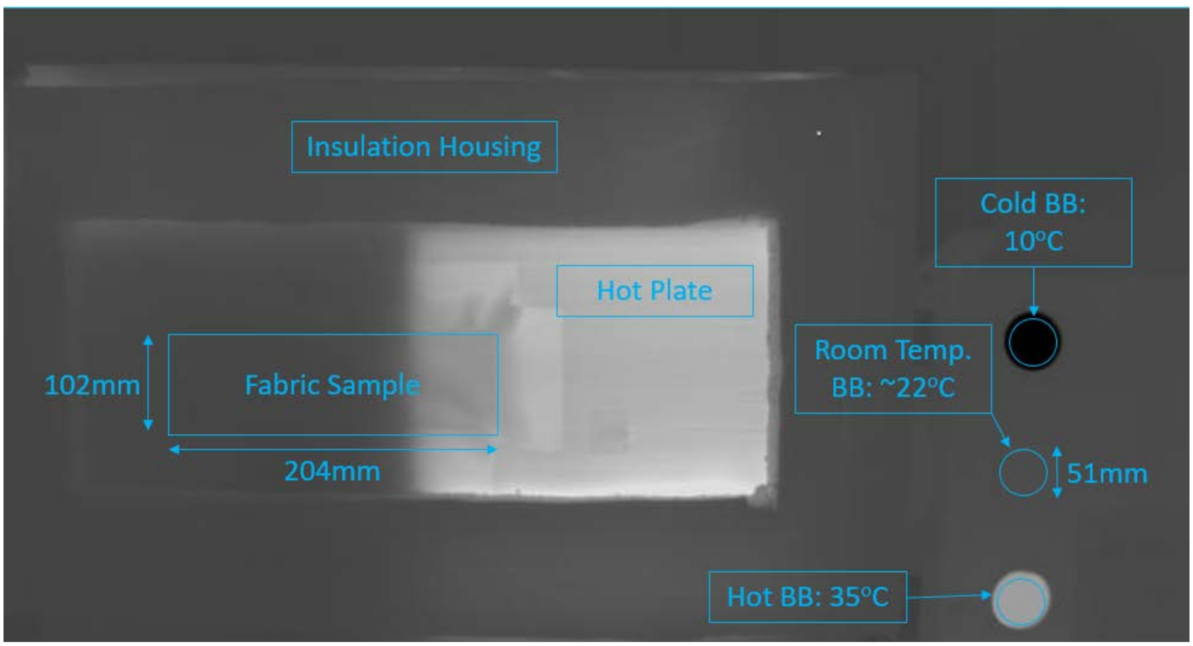

Figure 6. Thermal image of experimental test setup with components labeled. This is the control sample prior to attaching the heat sink. Note that the boxes in the figure are used to show the location of the important features in the experimental setup.

A FLIR SC6100 MWIR (3-5µm) camera was used to record experimental temperatures. Captured thermal IR images were calibrated using in-scene blackbodies (35 °C, ambient room temperature (22 °C), and 10 °C). By averaging the pixel intensity values over respective blackbody regions of interest (ROI). A linear calibration curve was created to map pixel intensity to a specific temperature. .

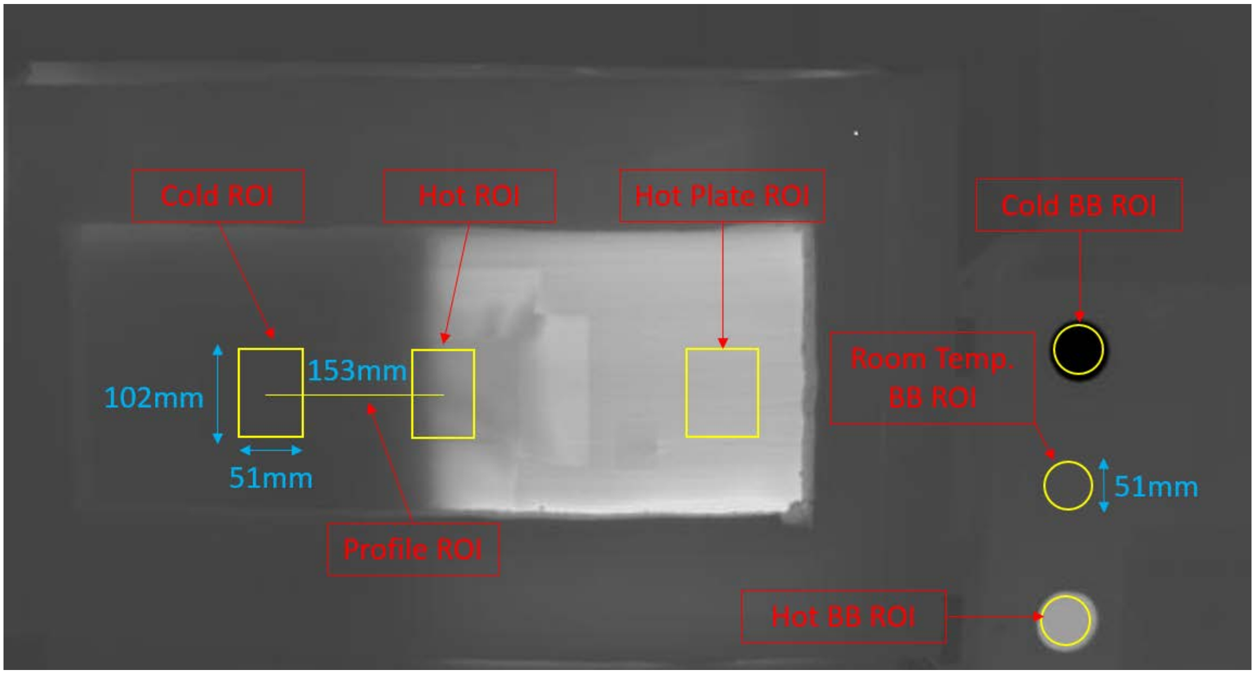

Figure 7. Thermal image of experimental test setup with ROI's labeled. This is the control sample prior to attaching the heat sink. Note that the boxes in the figure are the locations of the ROI's used by the thermal imaging software. The thermal imaging software averages the pixel intensity values over the specific ROI to determine the average temperature of the enclosed region.

Four materials were tested in triplicate for proof-of-concept, heatsink-controlled temperature distributions: a control consisting of only the 50/50 nylon/cotton ripstop fabric, and test samples consisting of the 50/50 nylon/cotton ripstop fabric adhered to either copper, aluminum, or carbon sheets. The outer fabric layer was attached to the conductive substrates via spray adhesive. Thickness statistics and thermal properties concerning the measured temperature distributions are given in Tables 1 and 2, respectively. Temperature profiles were recorded before and after test sample attachment to the cold plate. Each material was allowed to reach a steady state temperature prior to cold plate attachment. After attachment of the test samples to the cold plate, a 10-minute video of the temperature distribution was recorded. Temperature profiles were reevaluated after the 10-minute duration. Note that the test samples reached steady state equilibrium prior to the end of the 10 minute evaluation time.

Table 1. Material thicknesses.

Material	*Fabric Thickness [mm]*	*Metal Thickness [mm]*	*Glue Thickness [mm]*	*Total Thickness [mm]*
Control Fabric	0.656	--	--	0.656
Aluminum	0.656	0.027	0.030	0.713
Copper	0.656	0.018	0.047	0.721
Graphite	0.656	0.029	0.034	0.719

Table 2. Thermal properties for each material stack. The thermal conductivity presented is at 300 K. The thermal conductivity values for each of the materials were taken from references that used thin foil sheets of the material. Note that the XZ-plane is perpendicular to the heat source and the YZ-plane is parallel to the heat source, see Figure 2. [4, 5, 6]

Material	*Individual Layer Thermal Conductivity [W·m⁻¹·K⁻¹]*		*Individual Layer Thermal Resistance [K·W⁻¹]*		*Multi-Layer Material Thermal Resistance [K·W⁻¹]*	
	XZ-Plane	YZ-Plane	XZ-Plane	YZ-Plane	XZ-Plane	YZ-Plane
Control Fabric	$9.15\cdot10^{-4}$	$9.15\cdot10^{-4}$	3332.00	34455	3332.00	34455
Aluminum	234	234	0.32	$5.55\cdot10^{-3}$	3332.32	$5.55\cdot10^{-3}$
Copper	392	392	0.28	$2.21\cdot10^{-3}$	3332.28	$2.21\cdot10^{-3}$
Graphite	1223	7	0.06	$1.14\cdot10^{-3}$	3332.06	$1.14\cdot10^{-3}$

Results

The outer surface temperature of the multi-layered material, whose outer surface was a 50/50 cotton nylon blend for each test, was evaluated with a FLIR SC6100 MWIR (3-5µm) camera before and after cold plate coupling to the multi-layered material. For each material, a region of interest (ROI) was drawn over the material at the heat sink and source locations, see Figure 6. To evaluate the outer surface temperature, the pixel intensities were averaged and calibrated to a set of blackbodies. Average temperatures and relevant statistics are given in Table 3. The material with aluminum acting as the heat conduction medium proved to have the highest average temperature difference (-7.2^{o}C) compared to the average temperature difference of -1.5 ^{o}C for the Control.

Table 3. Average change in temperature before and after heat sink coupling to each material.

Material	*Average Δ T [^{o}C]*	*Multi-Layer Material Thermal Resistance [K·W⁻¹]*	
		XZ-Plane	YZ-Plane
Control	-1.5	3332.00	34455
Copper	-4.9	3332.32	$5.55\cdot10^{-3}$
Aluminum	-7.2	3332.28	$2.21\cdot10^{-3}$
Graphite	-4.9	3332.06	$1.14\cdot10^{-3}$

Table 4. Average ROI Statistics for each material before and after cold plate (CP) coupling. The temperature difference is the difference between the hotplate fabric ROI before and after cold plate coupling.

	Hot BB [°C]	***Room Temp. BB [°C]***	***Cold BB [°C]***	***Hot Plate Temp. [°C]***	***Cold ROI Fabric Temp. [°C]***	***Hot ROI Fabric Temp. [°C]***	***Δ T [°C]***	***Δ T Standard Deviation [°C]***
Control	34.9	21.9	10.0	33.8	21.5	37.8		
Control + CP	34.9	22.2	10.1	32.3	11.2	36.2	1.5	3.2
Copper	34.9	22.3	10.2	33.5	22.3	38.5		
Copper + CP	35.0	22.4	10.3	28.6	12.3	36.1	4.9	0.9
Aluminum	34.8	21.8	9.9	34.2	21.6	37.7		
Aluminum + CP	34.9	22.1	10.1	27.0	13.3	35.8	7.2	3.3
Graphite	34.9	22.3	10.1	33.1	24.0	38.0		
Graphite + CP	34.9	22.3	10.2	28.2	14.0	34.3	4.9	1.7

A line ROI was placed from the center of the Cold Fabric ROI to the center of the Hot Fabric ROI for every thermal image (e.g., Figure 6). The line profile was 153 mm long. For each sample, the temperature plots of the line ROIs were averaged before and after coupling the multi-layered material to the cold plate, Figures 7 – 8.

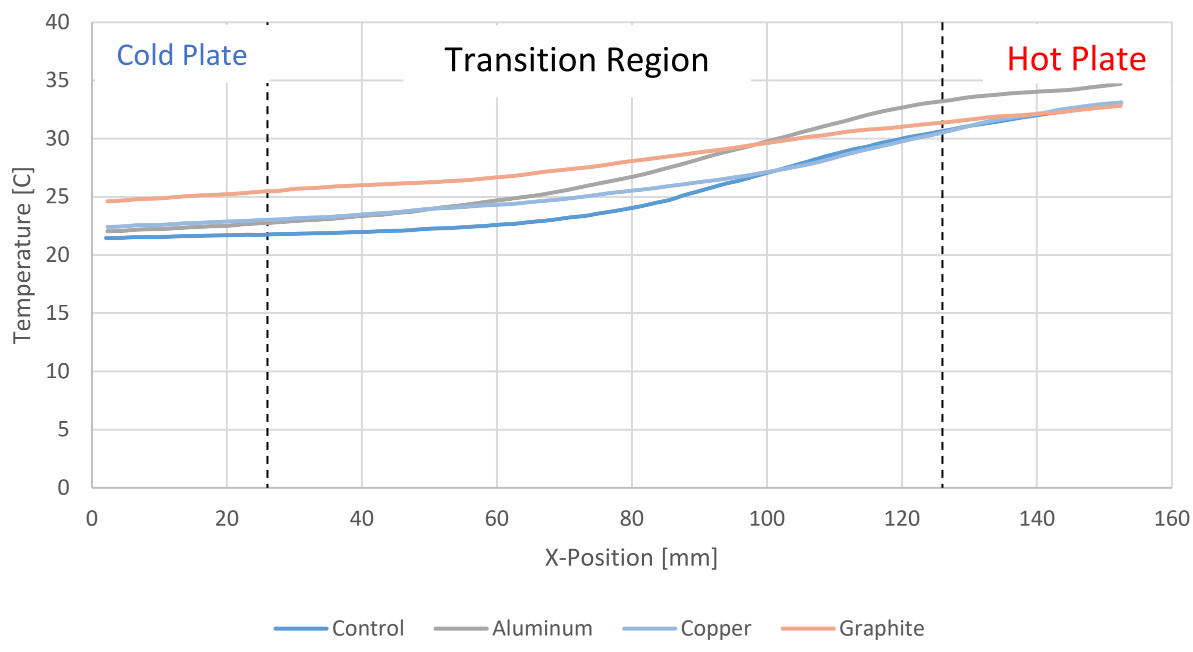

Figure 11. Averaged Line Plots of each of that materials before cold plate attachment.

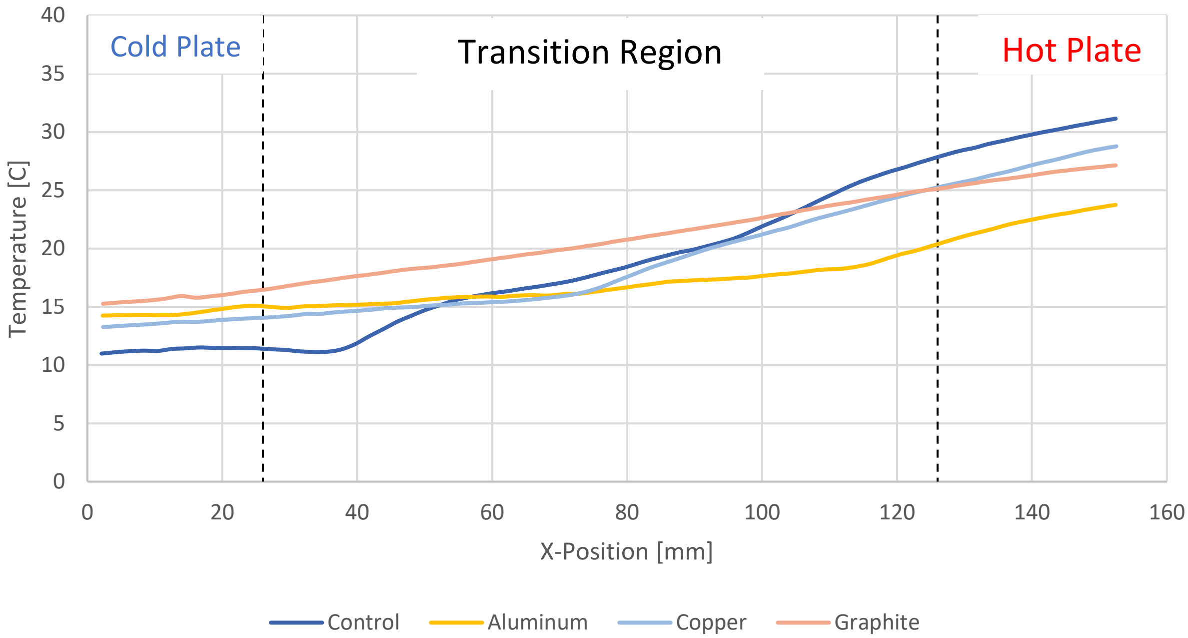

Figure 12. Averaged Line Plots of each of that materials after cold plate attachment.

In Figures 7 and 8, the control sample minimally reduces the outer surface temperature. Specifically, the control has an average difference in temperature of -1.5°C compared to -4.9 °C, -7.2 °C, and -4.9 °C for copper, aluminum, and graphite, respectively. This is indicative of less heat transfer in the YZ-plane from heat-source to cold plate.

Using Equation 6, the heat flux through the material was calculated in both the XZ and YZ planes (Table 5 and 6, respectively). For the calculation of the heat flux in the YZ plane, the median temperature of the layer was used.

Table 5. Average heat flux through the material in the XZ-plane. Note that a negative heat flux is indicative of energy leaving the outer surface of the material. A positive heat flux is indicative of energy entering the outer surface of the material.

Material	*Total Thermal Resistance [K·W^{-1}]]*	*Hot ROI Average ΔT [^{O}C]*	*Hot ROI Average Heat Flux [W·m^{-2}]*	*Cold ROI Average ΔT [^{O}C]*	*Cold ROI Average Heat Flux [W·m^{-2}]*
Control	3332.00	3.9	$-1.2 \cdot 10^{-3}$	21.2	$6.4 \cdot 10^{-3}$
Aluminum	3332.28	8.7	$-2.6 \cdot 10^{-3}$	23.3	$7.0 \cdot 10^{-3}$
Copper	3332.32	7.5	$-2.2 \cdot 10^{-3}$	22.3	$6.7 \cdot 10\text{-}^{3}$
Graphite	3332.06	6.1	$-1.8 \cdot 10^{-3}$	24.0	$7.2 \cdot 10^{-3}$

Table 6. Average heat flux through the material in the YZ-plane. Note that a negative heat flux is indicative of energy leaving the outer surface of the material. A positive heat flux is indicative of energy entering the outer surface of the material.

Material	*Total Thermal Resistance [$K \cdot W^{-1}$]]*	*Heat Sink Layer ΔT [^{O}C]*	*Heat Sink Layer Heat Flux [$W \cdot m^{-2}$]*	*Fabric ΔT [^{O}C]*	*Fabric Layer Heat Flux [$W \cdot m^{-2}$]*
Control	34455	NA	NA	33.7	$-9.8 \cdot 10^{-4}$
Aluminum	$2.21 \cdot 10^{-3}$	45.8	-8243	19.7	$-5.7 \cdot 10^{-4}$
Copper	$5.55 \cdot 10^{-3}$	46.1	-20845	21.2	$-6.1 \cdot 10^{-4}$
Graphite	$1.14 \cdot 10^{-3}$	44.3	-38889	19.3	$-5.6 \cdot 10^{-4}$

Discussion

The results show that a multi-layered material stack with a conductive substrate can provide a more efficient means of heat transmission between a cold plate (heat sink) and heat source. By adding metallic materials with high thermal conductivities to the layered material, the parallel heat flux increases along the fabric due to the reduction in thermal resistance between the heat source and cold source, resulting in a decrease in the outer surface temperature of the fabric. The data suggests that aluminum performed the best followed by graphite, copper, and the control with temperature differences of -7.2^{O}C, -4.9^{O}C, -4.9^{O}C, and -1.5^{O}C, respectively; however, the difference in temperature between the aluminum, copper, and graphite substrates are within one standard deviation. Thus, the different substrates are not statistically different, and more testing is required to effectively compare the three different substrates. The most likely cause of the apparent increased performance of aluminum is the quality of the coupling between the material stacks, the heatsinks, hot plate, and cold plate.

Conclusion

This report describes a series of experiments that provide proof of concept for heatsink-control of temperature fields within multi-layer materials consisting of a fabric and a thermally conductive substrate (e.g., a metallic layer). A general approach for control of heat transfer through multilayer materials is that of a system design that includes heat sinks as coupled or embedded layers. This approach is motivated by welding processes, where work piece temperatures are controlled by thermal contact to base plates, and by electronic system designs requiring thermal management. [1]

Although the materials tested were not optimum, the results demonstrate that a multi-layer material's temperature fields can be controlled by channeling the thermal energy from a heat-source to a cold plate via a thermally conductive substrate. This channeling of thermal energy from the heat-source to the cold plate reduces the temperature of the layers above the conductive substrate (e.g., fabric). This concept can be used to develop new technologies including wearable air conditioning (e.g., body heat) is removed via a conductive substrate to a cooling system. The next step in development will be to predict the 2-D temperature fields within a realistic multi-layer material via a parametric model that includes effects of contact resistance, heat reflection, convection, and radiation. After the development of a parametric model, the temperature fields can be simulated with realistic layers and optimized for specific developmental goals.

Acknowledgement

This work is supported by U.S. Special Operations Command, Special Operations Forces Acquisition, Technology, and Logistics (USSOCOM SOF AT&L).

References

1. S.G. Lambrakos, "Inverse Thermal Analysis of 304L Stainless Steel Laser Welds," J. Mater. Eng. And Perform., 22(8), 2141 (2013).
2. H.S. Carslaw and J.C. Jaegar "Conduction of Heat in Solids," Clarendon Press, Oxford, 2nd ed, 374, 1959.
3. J.R. Davis, "Properties of wrought aluminum alloys", metals handbook desk edition, ASM Int. (1998) 460-484
4. "Material Properties: OFHC Copper (UNS C10100/C10200)" ,Cryogenic Material Properties OFHC Copper. [online] Available at: https://trc.nist.gov/cryogenics/materials/OFHC%20Copper/OFHC_Copper_rev1.htm
5. Huang, Y., Su, Y., Guo, X., Guo, Q., Ouyang, Q., Zhang, G. and Zhang, D., 2017. "Fabrication and thermal conductivity of copper coated graphite film/aluminum composites for effective thermal management". Journal of Alloys and Compounds, 711, pp.22-30.